Eur. Phys. J. Plus (2016) **131**: 285
DOI 10.1140/epjp/i2016-16285-1

THE EUROPEAN PHYSICAL JOURNAL PLUS

Regular Article

Geometrical structure, stability and electronic properties of Au_nHg ($1 \leq n \leq 12$) clusters

Wei Wan[1,a] and Xiangjun Kuang[1,2,b]

[1] School of Science, Southwest University of Science and Technology, Mianyang, Sichuan, 621010, China
[2] College of Physics, Chongqing University, Chongqing, 400044, China

Received: 30 January 2016 / Revised: 17 July 2016
Published online: 24 August 2016 –

Abstract. The geometrical structures, relative stabilities, electronic properties and chemical hardness of Au_nHg (n = 1–12) clusters are systematically investigated using the density functional theory with relativistic all-electron methods. The optimized low-lying energy geometries exhibit two-dimensional and three-dimensional structures. Furthermore, all the lowest-energy structures of Au_nHg (n = 1–12) clusters favor planar geometries with slight distortion, in which the dopant Hg atom prefers to occupy a peripheral site with a lower coordination. The geometrical, electronic and chemical stabilities of the Au_nHg cluster with even number of valence electrons are higher than those of the neighboring Au_nHg cluster with odd number of valence electrons. Besides, 5*d* valence electrons of impurity Hg atom in the Au_nHg cluster hardly join in the orbital interactions compared with 5*d* valence electrons of corresponding Au atom in Au_{n+1} cluster. Au-Hg bonds in Au_nHg clusters are weaker and have more obviously ionic-like characteristics than the corresponding Au-Au bonds in Au_{n+1} clusters.

1 Introduction

In order to increase the number of variables for the purpose of material design and control, the doped gold clusters composed of two or more elements have also been studied extensively in the recent years [1–10]. The properties of doped gold clusters depend not only on the cluster size and geometry, but also on the cluster composition. Heterogeneous clusters are expected to show an extremely rich variety of catalytic behaviors as a function of the composition and chemical order. The exploration of the structure for these heterogeneous gold clusters may help to understand the catalytic activity of these catalysts and the interaction of the doped metal with the metal cluster. Among all these heterogeneous gold clusters, the transition metal atom doped gold clusters attract strong attention for their potential application in catalysis [11–14].

Mercury is not always considered as a typical transition metal because it does not possess partly filled *d* or *f* electron shells in the elemental or common oxidation states. Nevertheless, mercury including its congeners has a distinctive valence electronic configuration compared with other transition metals. The presence of impurity Hg atom or its congeners inevitably influences the stability and electronic structure of bare gold clusters. The Au_nHg clusters had been investigated using the density functional theory [15], and it was found that the equilibrium geometries prefer two-dimensional structures in the case of small cluster size. Moreover, theoretical calculations [16] also suggested that the energetically most favorable configuration is a linear structure with the Hg atom bonded to Au_2 dimer and the Au-Hg bond length is larger than the Au-Au bond. Recently, a density functional comparison study [17] was also presented on Au_{32} cluster doped with group IIB atoms, showing that the HOMO-LUMO gap of the Au_{32} cage doped with Zn, Cd or Hg atom is almost the same as that of the Au_{32} cage with high symmetry. Moreover, the mixed cation $[HgAuHg]^+$ is calculated at the *ab initio* level [18] and an analog of the known solid-state species Hg_3^{2+} is predicted. Several local minima and transition states are identified for larger Au_nHg_m clusters and the results are similar to the isoelectronic Au_n^{m-} anions. However, all these previous works are restricted on some special sizes, which cannot allow us to have an overview on the mercury-doped gold systems. Moreover, in contrast to the well-developed understanding of gold clusters doped with transition metal atoms, relatively less information is available about the structural and

[a] e-mail: wanwei@swust.edu.cn (corresponding author)
[b] e-mail: dxwlkj2012@sina.com

electronic properties of mercury-doped gold clusters. Hence, it is necessary to further and systematically investigate the structural, electronic and chemical properties of gold clusters doped with Hg. In this paper, the Au_nHg ($n = 1$–12) clusters have been investigated for the purpose to explore i) whether the geometries of mercury-doped gold clusters will be greatly different from pure gold clusters, ii) how the electronic and chemical properties of pure gold cluster will be changed obviously after doping a mercury atom and iii) moreover how the outer valence electrons of Hg atom will influence the electronic shells of gold clusters.

2 Computational methods

All geometrical optimizations of Au_nHg ($n = 1$–12) clusters are calculated using the spin-polarized density functional theory (DFT) in the DMOL3 program package [19–21]. The generalized gradient approximation (GGA) in the Becke exchange plus Perdew correlation (BP) [22,23] functional is chosen in the calculations. A double-numerical basis set including *d*-polarization functions (DNP) are adopted for the description of the electronic wave functions. Due to the obvious influence of scalar relativistic effect on the properties of gold clusters [24–32], the all-electron scalar relativistic (AER) method is adopted. Meanwhile, the convergence criteria are set with 0.002 Ha/Å for the forces, 0.005 Å for the displacement, and 10^{-5} Ha for the energy change, respectively.

In order to get the initial structures of Au_nHg ($n = 1$–12) clusters, we first optimized the structures of pure gold clusters considering previous works [33–36]. Then, based on these optimized equilibrium geometries of pure gold clusters, the possible initial structures of Au_nHg clusters can be constructed by substituting Hg atom for one gold atom of the Au_{n+1} cluster at every nonequivalent site or by adding Hg atom directly on each possible nonequivalent site of Au_n cluster. All these initial structures including one-, two-, and three-dimensional geometries are fully optimized by relaxing the atomic positions until the force acting on each atom vanishes (typically $|F_i| \leq 0.002$ Ha/Å) and the total energy achieves the minimum. During the structure relaxation, the spin multiplicity will be considered at least 2, 4 and 6 for odd-electrons Au_nHg clusters ($n = 1$, 3, 5, 7, 9 and 11) and 1, 3, 5 for even-electrons Au_nHg clusters ($n = 2$, 4, 6, 8, 10 and 12). If the total energy decreases with the increasing of spin multiplicity, the high spin state will be considered until the energy minimum with respect to the spin multiplicity is reached. In addition, the stability of the optimized geometry is confirmed without any imaginary frequency by computing vibrational frequencies at the same level of theory.

To check the intrinsic reliability of the computational method, some test calculations have been performed. For Au_2 dimer, our calculated values of the bond-length, dissociation energy, vertical ionization potential and vibrational frequency are 2.489 Å, 2.296 eV, 9.302 eV and 181.5 cm^{-1}, respectively, which are in good agreement with the corresponding experimental results [37–41] of 2.473 Å, 2.29 eV, 9.200 eV and 190.9 cm^{-1}. Meanwhile, for AuHg dimer, the bond-length of 2.626 Å and dissociation energy of 0.757 eV are close to previous theoretical calculation results [42] of 2.710 Å, and 0.670 eV. Furthermore, for $AuHg^+$ dimer, the bond-length of 2.554 Å and vibrational frequency of 155.3 cm^{-1} are also well consistent with previous theoretical calculation values of 2.590 Å and 147 cm^{-1} [43]. Thus, it is confident that the adopted computational method is reliable and accurate enough for the study of Au_nHg ($n = 1$–12) clusters.

3 Results and discussions

3.1 Equilibrium geometries

As is shown in fig. 1, the lowest-energy geometries and some typical low-lying geometries of Au_{n+1} and Au_nHg ($n = 1$–12) clusters are plotted according to the sequence of energies from low to high. Moreover, the symmetry, electronic state and energy difference between the lowest energy structure and its isomer are also indicated in this figure.

- AuHg. The lowest-energy geometry of the AuHg cluster is a linear structure with C_{∞_v} symmetry, and it can be generated by substituting Hg atom for one gold atom of the Au_2 cluster.
- Au_2Hg. The lowest-energy geometry of the Au_2Hg cluster is also a linear structure generated by bonding Hg atom with one gold atom of the Au_2 cluster. The linear structure generated by bonding the Hg atom with two gold atoms at two sides and the triangular structure produced by substituting the Hg atom for one gold atom of the Au_3 cluster are isomers with higher energy.
- Au_3Hg. Similar to the pure Au_4 cluster, the lowest-energy geometry 3a and the metastable geometry 3b for the Au_3Hg cluster are rhombus structures with C_{2v} symmetry. These isomers are generated by substituting the Hg atom with one gold atom of the Au_4 cluster at doubly and triply coordinated sites, respectively. Other structures (3c and 3d) generated by bonding the Hg atom directly with the Au_3 cluster at the site of the same plane or above the plane of the Au_3 cluster are low-lying geometric isomers with higher energy.

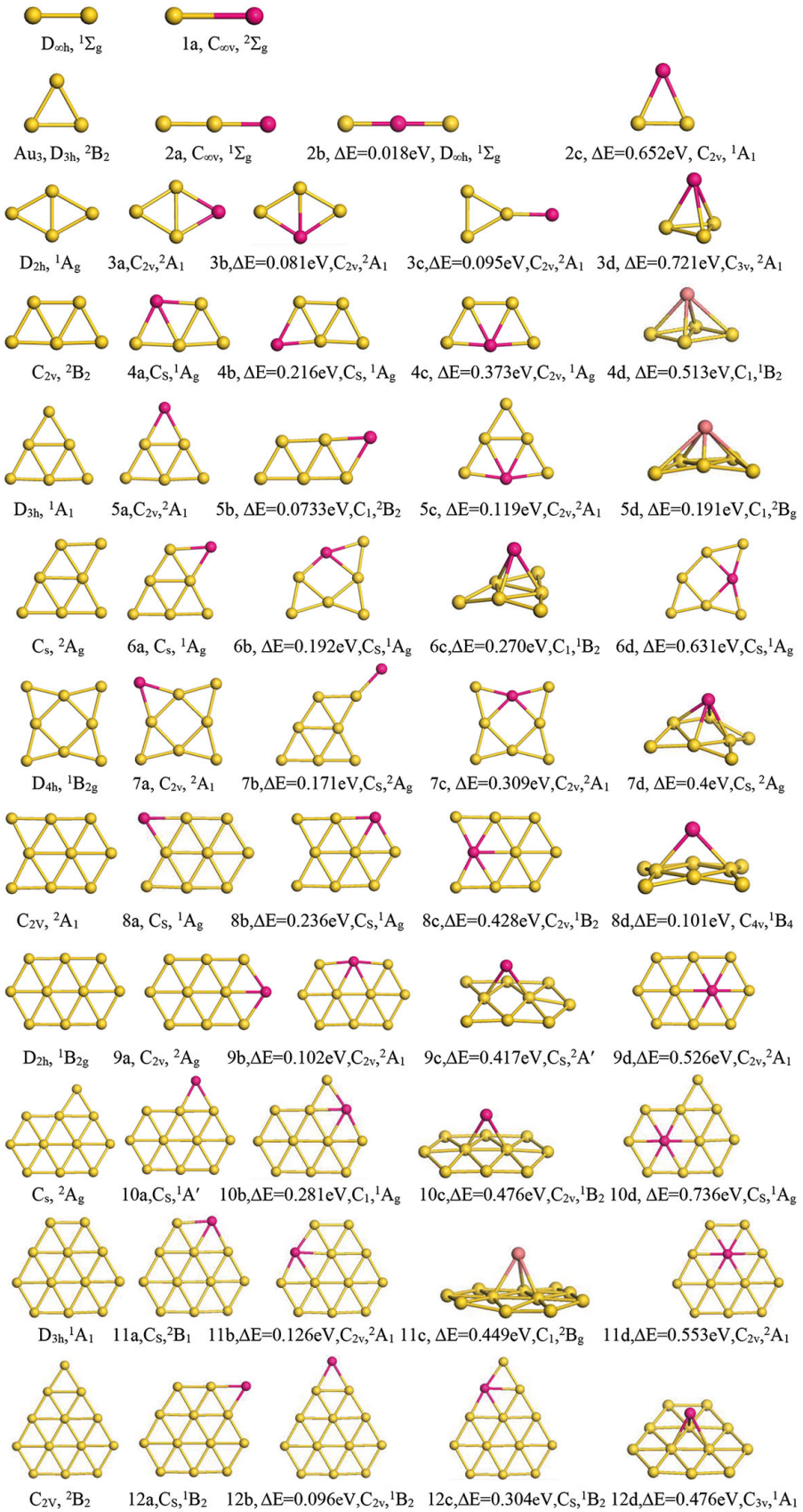

Fig. 1. Optimized geometries for Au_nHg (n = 1–12) clusters and the corresponding pure gold clusters. The golden and red balls represent Au and Hg atoms, respectively.

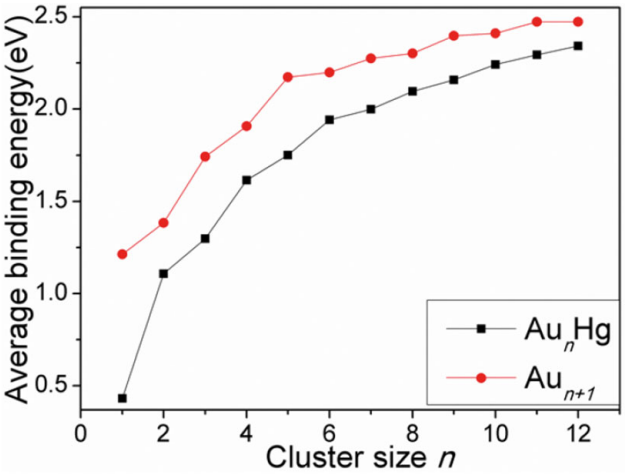

Fig. 2. Size dependence of the average binding energy for the lowest structures of Au_nHg clusters and Au_{n+1} clusters.

- Au_4Hg. Based on the trapezoid structure of the pure Au_5 cluster, the lowest-energy structure (4a) and two isomers (4b and 4c) are obtained by substituting the Hg atom with one gold atom at the triply, doubly and quadruply coordinated sites of the Au_5 cluster, respectively. The geometry (4d) generated by bonding the Hg atom above the plane of the Au_4 cluster is the low-lying geometric isomer with higher energy of 0.513 eV.
- Au_5Hg. The lowest-energy geometry of the Au_5Hg cluster is the structure of 5a generated by substituting the Hg atom with one Au atom at the doubly coordinated site of the Au_6 cluster, which is a big triangle similar to the Au_6 cluster. The isomers 5b and 5d can be obtained by bonding the Hg atom with the Au_5 cluster in the same plane or above the plane as double bond and quintuple bond, respectively. Additionally, the isomer 5c is generated by substituting the Hg atom with one Au atom at the quadruply coordinated site of the Au_6 cluster.
- Au_6Hg. Similar to the structure of the Au_7 cluster, the lowest-energy geometry of the Au_6Hg cluster (6a) is produced by substituting the Hg atom with one Au atom at the doubly coordinated site of the Au_7 cluster. The structures 6b and 6d obtained by replacing the Au atom with the Hg atom at triply and quintuply coordinated site in the Au_7 cluster are isomers. The 3D structure (6c) generated by bonding the Hg atom with the Au atom above the plane of the Au_6 cluster is another isomer for the Au_6Hg cluster.
- Au_7Hg. The tera-edge-capped rhombus geometry (7a) produced by substituting the Hg atom with one Au atom at the doubly coordinated site of the Au_8 cluster is the lowest-energy structure of the Au_7Hg cluster. The isomer 7c is also a tera-edge-capped rhombus generated by substituting the Hg atom for one Au atom at the quadruply coordinated site of the Au_8 cluster. Other structures (7b and 7d) generated by bonding the Hg atom directly with the Au_7 cluster at the site of the same plane or by capping the Hg atom above the plane of the Au_7 cluster are low-lying geometric isomers with higher energy. In 7d geometry, the structure is bent and up-swelled obviously after optimization.

With regard to the Au_nHg ($n = 8$–12) clusters, some similar characteristics of geometrical structure can be observed clearly. The lowest-energy geometries of these clusters may be generated by substituting the Hg atom with one gold atom of the Au_{n+1} cluster at the triply coordinated site or by bonding Hg with the Au_n cluster as two-fold bond, the dopant Hg atom is located at the edge of planar structures. Compared with corresponding pure gold cluster, the lowest-energy geometries of the Au_nHg clusters are distorted slightly and still keep the planar structures. This situation can also be seen in previous works and is believed to be the reflection of strong scalar relativistic effects in gold clusters [24–32]. For the 3D initial structures generated by capping one Hg atom above the plane of the Au_n cluster, the plane will be bent and up-swelled slightly after optimization, the distortion can still be observed clearly. In particular, the lowest-energy geometries of Au_2Hg and Au_4Hg in our work are in good agreement with previous studies on Au_nHg_m clusters [15–18].

3.2 Stabilities

In order to investigate the cluster stabilities, the average binding energy and second-order difference of energy including the zero-point-energy (ZPE) corrections estimated with the respective functional for pure Au_{n+1} clusters and Au_nHg clusters are displayed in figs. 2 and 3, where we define:

$$E_b(\mathrm{Au}_n\mathrm{Hg}) = [nE(\mathrm{Au}) + E(\mathrm{Hg}) - E(\mathrm{Au}_n\mathrm{Hg})]/(n+1) \quad (1)$$

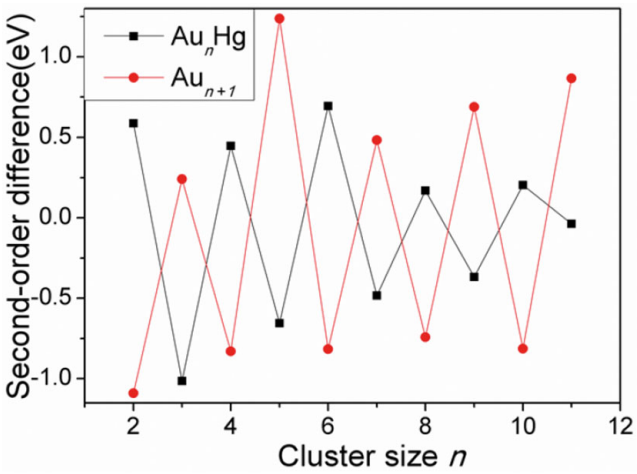

Fig. 3. Size dependence of the second-order difference energy for the lowest structures of Au_nHg clusters and Au_{n+1} clusters.

$$E_b(Au_{n+1}) = [(n+1)E(Au) - E(Au_{n+1})]/(n+1), \quad (2)$$

$$\Delta_2 E(n) = E(Au_{n+1}) + E(Au_{n-1}) - 2E(Au_n) \quad (3)$$

$$\Delta_2 E(n) = E(Au_{n+1}Hg) + E(Au_{n-1}Hg) - 2E(Au_nHg). \quad (4)$$

From fig. 2, we can find that with increasing size of clusters, the average binding energy of the Au_{n+1} cluster and the Au_nHg cluster increases gradually and reaches the maximum value at Au_{13} cluster and $Au_{12}Hg$ cluster respectively, the variation tendency of the average binding energy for pure Au_{n+1} clusters and Au_nHg clusters is similar. Furthermore, the average binding energy of Au_nHg cluster is obviously smaller than that of corresponding pure Au_{n+1} cluster, the average binding energy difference between Au_nHg and corresponding Au_{n+1} cluster becomes small with increasing size. It is inferred that the doped Hg atom might weaken the stability of Au_nHg cluster energetically. With the increasing size of clusters, the stability of the Au_nHg cluster increases gradually like the increasing stability of pure gold cluster, and the stability weakening effect of the doped Hg atom will be decreased gradually.

The second-order difference energy is a sensitive parameter to reveal the relative stability of cluster. As is shown in fig. 3, the obvious odd-even oscillations of second-order difference energy for Au_nHg and Au_{n+1} clusters can be observed clearly. For pure Au_{n+1} clusters, the second-order difference energy for odd-numbered Au_{n+1} cluster is larger than that for adjacent even-numbered Au_{n+1} cluster, indicating that the odd-numbered Au_{n+1} cluster is relatively more stable than the adjacent even numbered Au_{n+1} cluster. After doping the Hg atom, the second-order difference energy for even-numbered Au_nHg cluster is larger than that for adjacent odd-numbered Au_nHg cluster, the even-numbered Au_nHg cluster are relatively more stable than the adjacent odd-numbered Au_nHg cluster. The odd-even alteration of relative stability for Au_{n+1} clusters and Au_nHg clusters is pronounced.

The fragmentation energies between Au_n and Hg in the Au_nHg cluster and between Au_n and corresponding Au in the Au_{n+1} cluster (including ZPE corrections estimated with the respective functional) are defined as follows:

$$E_f(Au_{n+1}) = [E(Au_n) + E(Au) - E(Au_{n+1})] \quad (5)$$

$$E_f(Au_nHg) = [E(Au_{n-1}Hg) + E(Au) - E(Au_nHg)]. \quad (6)$$

The fragmentation energy is a useful parameter which reveals the interaction between the two parts in the cluster. From the calculation results shown in fig. 4, the odd-even oscillations of fragmentation energy for Au_nHg and Au_{n+1} clusters can be observed again. It is suggested that the Au_n-Au interaction in odd-numbered Au_{n+1} cluster is stronger than that in adjacent even-numbered Au_{n+1} cluster, and the Au_n-Hg interaction in even-numbered Au_nHg cluster is stronger than that in adjacent odd-numbered Au_nHg cluster. That is to say, after doping the Hg atom, the stronger Au_n-Au interaction in odd-numbered Au_{n+1} cluster becomes the weaker Au_n-Hg interaction in the odd-numbered Au_nHg cluster, and the weaker Au_n-Au interaction in the even-numbered Au_{n+1} cluster becomes the stronger Au_n-Hg interaction in the even-numbered Au_nHg cluster. The odd-even alterations of Au_n-Au interaction in Au_{n+1} clusters and Au_n-Hg interaction in Au_nHg clusters are also presented clearly.

In addition to above parameters, the chemical hardness is also regarded as a crucial parameter which estimates the reactivity of a system. In density functional theory, the chemical hardness (η) of a system is defined as [44]

$$\boldsymbol{\eta} = (VIP - VEA)/2, \quad (7)$$

where VIP and VEA are vertical ionization potential and the vertical electron affinity including ZPE corrections estimated with the respective functional, respectively.

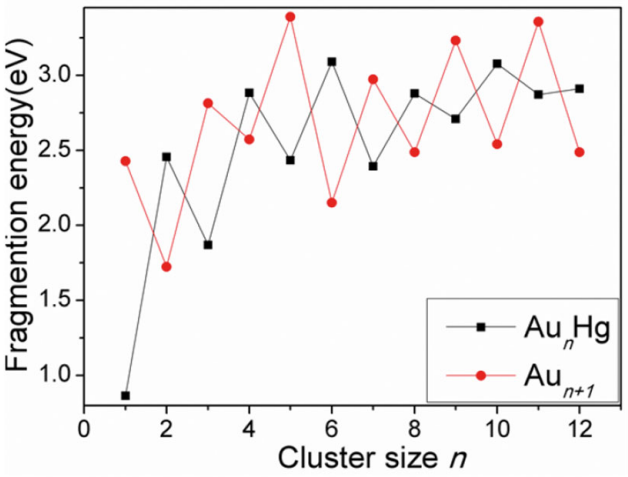

Fig. 4. Size dependence of fragmentation energies for the lowest structures of Au_nHg clusters and Au_{n+1} clusters.

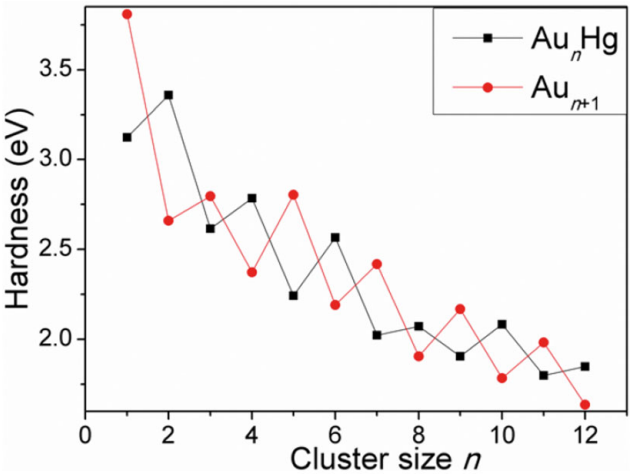

Fig. 5. Size dependence of the chemical hardness for the lowest structures of Au_nHg clusters and Au_{n+1} clusters.

As is shown in fig. 5, the chemical hardness of the even-numbered Au_nHg cluster is higher than those of the neighboring odd-numbered Au_nHg cluster and the corresponding Au_{n+1} cluster, and moreover, the chemical hardness of the odd-numbered Au_nHg cluster is lower than that of the neighboring even-numbered Au_nHg cluster and corresponding Au_{n+1} cluster. According to the principle of maximum hardness (PMH) [45,46], the even-numbered Au_nHg cluster is more stable chemically and less reactive than the neighboring odd-numbered Au_nHg cluster and corresponding Au_{n+1} cluster, the odd-numbered Au_nHg cluster is less stable chemically and more reactive than the neighboring even-numbered Au_nHg cluster and corresponding Au_{n+1} cluster, implying that the odd-even alteration of chemical stability pattern for host gold cluster takes place after doping Hg atom.

3.3 Electronic properties

HOMO-LUMO gap (HLG) is often used to test the electronic stability of a cluster. The larger of HLG, the higher energy is required to excite the electrons from valence band to conduction band, corresponding to higher stability of electronic structure. At first glance of the results displayed in fig. 6, the odd-even oscillations of HLG similar with fragmentation energy and chemical hardness can be seen clearly, indicating that the electronic structure of odd-numbered Au_{n+1} cluster is more stable than that of the adjacent even-numbered Au_{n+1} cluster, and the electronic structure of even-numbered Au_nHg cluster is more stable than that of the adjacent odd-numbered Au_nHg cluster after doping the Hg atom.

Throughout above discussions, the odd-even oscillations of second-order difference of energy, fragmentation energy, chemical hardness and HLG for Au_{n+1} clusters and Au_nHg clusters are observed clearly. This picture also can be seen in gold cluster [47], silver cluster [48], copper clusters [49], gold-based heterogeneous cluster [50–52] and the adsorption behavior of gold cluster toward small molecules [53–56]. It is the reflection of spin-pairing effect well known for coinage

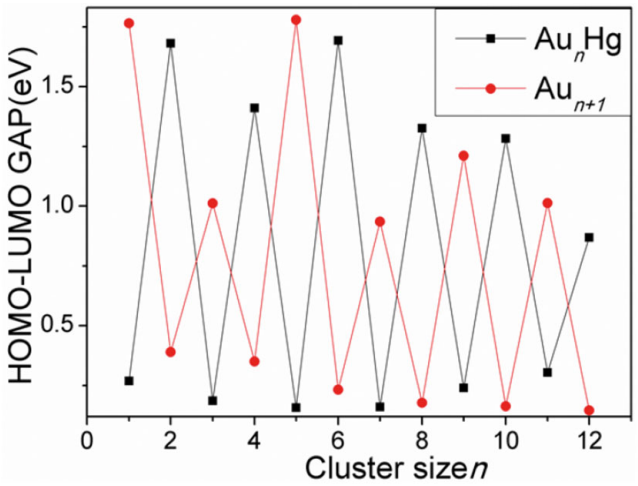

Fig. 6. Size dependence of the HOMO-LUMO gap for the lowest structures of Au_nHg clusters and Au_{n+1} clusters.

Table 1. Calculated charges populations of Hg5d, 6s, 6p orbitals in Au_nHg clusters and corresponding Au5d, 6s, 6p orbitals in Au_{n+1} clusters.

	Au_nHg				Au_{n+1}			
n	5d	6s	6p	Hg	5d	6s	6p	Au
1	9.967	1.680	0.216	0.137	9.870	0.863	0.069	0.198
2	9.966	1.711	0.139	0.184	9.782	0.871	0.193	0.154
3	9.954	1.596	0.322	0.128	9.760	0.802	0.337	0.101
4	9.939	1.461	0.438	0.162	9.622	0.879	0.440	0.059
5	9.946	1.632	0.303	0.119	9.664	0.889	0.408	0.039
6	9.965	1.751	0.146	0.138	9.556	0.824	0.542	0.078
7	9.946	1.588	0.302	0.164	9.620	0.914	0.451	0.015
8	9.949	1.614	0.301	0.136	9.526	0.786	0.602	0.086
9	9.934	1.477	0.438	0.151	9.516	0.775	0.613	0.096
10	9.947	1.625	0.285	0.143	9.473	0.817	0.639	0.071
11	9.932	1.477	0.439	0.152	9.471	0.827	0.642	0.060
12	9.948	1.643	0.271	0.138	9.473	0.834	0.630	0.063

metal clusters and alkali metal clusters [57,58]. As coinage metal atoms possess filled d-shells, their electronic structures are largely determined by the half-filled bands of nearly free s electrons. Thus, it is not surprising that all coinage metal clusters exhibit size dependence odd-even oscillations of properties that are similar to those observed in alkali metal clusters.

To further investigate the influence of dopant Hg atom on the electronic structure of host gold clusters, a detailed Mulliken population analysis has been performed and the results are summarized in table 1. Here, the valence electrons configurations of free Au $5d^{10}6s^1$ and Hg $5d^{10}6s^2$ are presented for comparison. As can be seen in table 1, the Hg atom obviously has positive charge, indicating that the charge transfers from the Hg atom to Au atoms in the Au_nHg cluster, the Hg atom acts as an electronic donor, and most Au atoms act as electronic hosts. Moreover, for the impurity Hg atom, the 5s states lose 0.320–0.539 electrons, while the 6p states receive 0.139–0.439 electrons in Au_nHg clusters. Especially, the contribution of the 5d states is 0.033–0.068 electrons as nearly zero, which can be neglected. It is suggested that there is the strong s-p hybridization in the Hg atom or between the Hg atom and Au atoms in Au_nHg clusters, which differs from the *spd* hybridization in the corresponding Au atom of Au_{n+1} clusters. Besides, 9.932–9.967 electrons occupy the 5d obital of Hg atoms in Au_nHg clusters, signifying that the 5d obital of dopant Hg atom as well as the 5d obital of Au atoms in Au_{n+1} clusters is dominant core obitals. This characteristic of electronic properties for Hg-doped gold clusters is different from that of other transition metal doped gold clusters [1,59].

In order to understand the chemical bonding natures and the odd-even oscillation phenomena of stability of Au_nHg, the highest occupied molecular orbital (HOMO) and the lowest unoccupied molecular orbital (LUMO) with their energy level for several representative Au_nHg clusters are plotted in fig. 7. As is shown in fig. 7, for $Au_{10}Hg$ cluster with even number of valence electrons, the HOMO are a doubly degenerate state as well as LUMO. Furthermore, the energy level of HOMO of $Au_{10}Hg$ cluster is obviously lower than that of HOMO of adjacent Au_9Hg cluster and $Au_{11}Hg$ cluster. The valence electrons with reverse spins in even-numbered Au_nHg cluster doubly occupy the HOMO, and therefore the stability of even-numbered Au_nHg cluster is higher that of odd-numbered one. Additionally, owing to

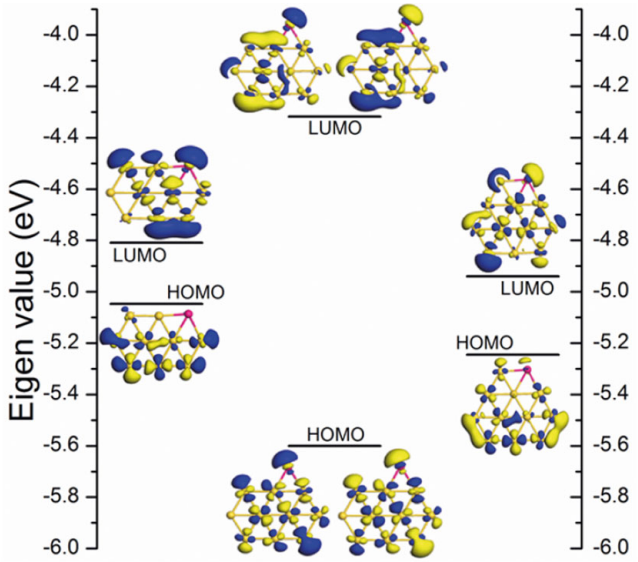

Fig. 7. Some representative HOMO and LUMO for the lowest-energy geometries of Au_nHg clusters.

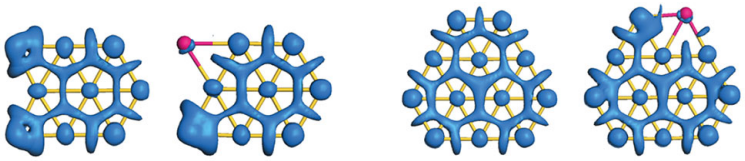

Fig. 8. Comparison on deformation electron density of Au_nHg clusters and corresponding Au_{n+1} clusters for the lowest-energy structures with surface isovalue $0.023\,e/Å^3$ for molecular orbital plotting.

the presence of dopant Hg atom, the distribution of electron cloud of Au_nHg cluster is no longer symmetric, uniform and well mixed, namely the delocalization of HOMO and LUMO is impaired markedly. Meanwhile, the overlap of electron cloud between the frontier orbitals of Hg and Au in Au_nHg cluster can be observed and the pronounced *s-p* hybridization is obvious just as we thought.

Next, we shall further illustrate the charge transfer between the dopant Hg and Au atoms, the electron deformation densities of $Au_{9,11}Hg$ clusters and corresponding $Au_{10,12}$ clusters as examples are plotted in fig. 8 and the blue area represents electron accumulations. In fig. 7, the electron deformation density in $Au_{9,11}Hg$ clusters exhibits that just a few electrons distribute around the Hg atom and in the interval of Au-Hg bonds compared with electron distributions around adjacent Au atoms and in the interval of Au-Au bonds. The ionic-like characteristic in the Au-Hg bond is more obvious than that in the corresponding Au-Au bond. Compared with pure gold clusters, the electron accumulation between the Hg and Au atoms markedly decreases after the impurity Hg atom replaces an Au atom, suggesting that the Au-Hg interaction in Au_nHg cluster is weaker than the corresponding Au-Au interaction in Au_{n+1} cluster. Furthermore, previous work [60] indicated that dispersion interactions in small mercury clusters is significant, it is inferred that this dispersion interactions may also exist in Au_nHg clusters and the mercury can be considered as a weakly interacting adduct and not a covalently bound moiety.

4 Conclusions

In this paper, an all-electron scalar relativistic calculation on Au_nHg (n = 1–12) clusters has been performed using density functional theory with the generalized gradient approximation at PW91 level. The main conclusions are summarized as follows:

1) All the lowest-energy structures of Au_nHg (n = 1–12) clusters favor planar geometries with slight distortion, in which the dopant Hg atom prefers to occupy a peripheral site with lower coordination.
2) The odd-even oscillations of fragmentation energies, second-order difference of energies, chemical hardness and HOMO-LUMO energy gaps for Au_nHg clusters are displayed obviously, indicating that the even-numbered Au_nHg cluster with even number of valence electrons is more stable and less reactive than the adjacent odd-numbered Au_nHg cluster with odd number of valence electrons.

3) There are strong *s-p* orbital interactions in the Hg atom or between the Hg atom and Au atoms in Au_nHg clusters, which differs from the *spd* orbital interactions in the corresponding Au in Au_{n+1} clusters. The Au-Hg bond in the Au_nHg cluster is weaker and has more obviously ionic-like characteristics than the corresponding Au-Au bond in the Au_{n+1} cluster.

This work is supported by the Natural Science Foundation of Department of Education of Sichuan Province. No.14zd1116.

References

1. D.W. Yuan, Y. Wang, Z. Zeng, J. Chem. Phys. **122**, 114310 (2005).
2. J.L. Rao, G.K. Chaitanya, S. Basavaraja, K. Bhanuprakash, A. Venkataramana, J. Mol. Struct. THEOCHEM **803**, 89 (2007).
3. W. Bouwen, F. Vanhoutte, F. Despa, S. Bouckaert, S. Neukermans, L.T. Kuhn, H. Weidele, P. Lievens, R.E. Silverans, Chem. Phys. Lett. **314**, 227 (1999).
4. L.M. Wang, J. Bai, A. Lechtken, W. Huang, D. Schooss, M.M. Kappes, X.C. Zeng, L.S. Wang, Phys. Rev. B **79**, 033413 (2009).
5. X. Li, B. Kiran, L.F. Cui, L.S. Wang, Phys. Rev. Lett. **95**, 253401 (2005).
6. B.R. Sahu, G. Maofa, L. Kleinman, Phys. Rev. B **67**, 115420 (2003).
7. X.J. Li, K.H. Su, Theor. Chem. Acc. **124**, 345 (2009).
8. G. Rossi, R. Ferrando, A. Rapallo, A. Fortunelli, B.C. Curley, L.D. Lloyd, R.L. Johnston, J. Chem. Phys. **122**, 194309 (2005).
9. S.F. Li, X.L. Xue, Y. Jia, G.F. Zhao, M.F. Zhang, X.G. Gong, Phys. Rev. B **73**, 165401 (2006).
10. E. Cottancin, J. Lerme, M. Gaudry, M. Pellarin, J.L. Vialle, M. Broyer, Phys. Rev. B **62**, 5179 (2000).
11. H. Tada, F. Suzuki, S. Ito, T. Akita, K. Tanaka, T. Kawahara, H. Kobayashi, J. Phys. Chem. B **106**, 8714 (2002).
12. K. Koszinowski, D. Schroder, H. Schwarz, Chem. Phys. Chem. **4**, 1233 (2003).
13. K. Koszinowski, D. Schroder, H. Schwarz, Organometallics **23**, 1132 (2004).
14. K. Koszinowski, D. Schroder, H. Schwarz, J. Am. Chem. Soc. **125**, 3676 (2003).
15. E. Rykova, A. Zaitsevskii, N. Mosyagin, T. Isaev, A. Titov, J. Chem. Phys. **125**, 241102 (2006).
16. E.M. Fernández, L.C. Balbás, Phys. Chem. Chem. Phys. **13**, 20863 (2011).
17. D. Manna, T. Jayasekharan, T.K. Ghanty, J. Phys. Chem. C **117**, 18777 (2013).
18. P. Zaleski-Ejgierd, P. Pyykko, J. Phys. Chem. A **113**, 12380 (2009).
19. Y.S. Lee, W.C. Ermler, K.S. Pitzer, J. Chem. Phys. **67**, 5861 (1997).
20. B. Delley, J. Chem. Phys. **113**, 7756 (2000).
21. B. Delley, J. Chem. Phys. **92**, 508 (1990).
22. A.D. Becke, J. Chem. Phys. **88**, 2547 (1988).
23. J.P. Perdew, Y. Wang, Phys. Rev. B **45**, 13244 (1992).
24. J. Autschbach, S. Siekierski, M. Seth, P. Schwerdtfeger, W. Schwarz, J. Comp. Chem. **23**, 804 (2002).
25. S.N. Datta, C.S. Ewig, J.R.V. Wazer, Chem. Phys. Lett. **57**, 83 (1978).
26. W.J. Stevens, M. Krauss, H. Basch, P.G. Jasien, Can. J. Chem. **70**, 612 (1992).
27. S. Wildman, G. Dilabio, P. Christiansen, J. Chem. Phys. **107**, 9975 (1997).
28. P.K. Jain, Struct. Chem. **16**, 421 (2005).
29. J. Wang, G. Wang, J. Zhao, Phys. Rev. B **66**, 035418 (2002).
30. S. Gilb, P. Weis, F. Furche, R. Ahlrichs, M.M. Kappes, J. Chem. Phys. **116**, 4094 (2002).
31. R. Wesendrup, T. Hunt, P. Schwerdtfeger, J. Chem. Phys. **112**, 9356 (2000).
32. E.M. Fernández, J.M. Soler, I.L. Garzón, L.C. Balbás, Phys. Rev. B **70**, 165403 (2004).
33. A. Deka, R.C. Deka, J. Mol. Struct. THEOCHEM **870**, 83 (2008).
34. H.P. Mao, H.Y. Wang, Y. Ni, G.L. Xu, Acta. Phys. Sin. **53**, 1766 (2004).
35. H. Myoung, M. Ge, B.R. Sahu, P. Tarakeswar, K.S. Kim, J. Chem. Phys. **107**, 9994 (2003).
36. H. Hakkinen, U. Landman, Phys. Rev. B **62**, 2287 (2000).
37. S. Simard, P. Hackett, J. Mol. Spectrosc. **142**, 310 (1990).
38. J. Ho, K.M. Ervin, W. Lineberger, J. Chem. Phys. **93**, 6987 (1990).
39. L. Ames, R. Barrow, Trans. Faraday Soc. **63**, 39 (1967).
40. K.P. Huber, G. Herzberg, *Constants of diatomic molecules* (Van Nostrand Reinhold, New York, 1979).
41. C. Jackslath, I. Rabin, W. Schulze, B. Bunsenges, Phys. Chem. **96**, 1200 (1992).
42. V. Pershina, J. Anton, T. Bastug, Eur. Phys. J. D **45**, 87 (2007).
43. R. Wesendrup, J.K. Laerdahl, P. Schwerdtfeger, J. Chem. Phys. **110**, 9457 (1999).
44. K. Fukui, Science **218**, 747 (1982).
45. L. Guo, J. Alloys Comp. **498**, 121 (2010).
46. J.G. He, K.G. Wu, C.P. Liu, R.G. Sa, Chem. Phys. Lett. **483**, 30 (2009).
47. H. Hakkinen, U. Landman, Phys. Rev. B **62**, R2287 (2000).
48. H.L. Zhang, D.X. Tian, Comput. Mater. Sci. **42**, 46 (2008).

49. G.H. Guvelioglu, P.P. Ma, X.Y. He, R.C. Forrey, H.S. Cheng, Phys. Rev. B **73**, 155436 (2006).
50. X.J. Kuang, X.Q. Wang, G.B. Liu, J. Alloys Comp. **570**, 46 (2013).
51. X.J. Kuang, X.Q. Wang, G.B. Liu, Eur. Phys. J. D **63**, 111 (2011).
52. X.J. Kuang, X.Q. Wang, G.B. Liu, Trans. Met. Chem. **36**, 643 (2011).
53. X.J. Kuang, X.Q. Wang, G.B. Liu, App. Surf. Sci. **257**, 6546 (2011).
54. X.J. Kuang, X.Q. Wang, G.B. Liu, Catal. Lett. **137**, 247 (2010).
55. X.J. Kuang, X.Q. Wang, G.B. Liu, J. Mol. Model. **17**, 2005 (2011).
56. S. Phala, G. Klatt, E.V. Steen, Chem. Phys. Lett. **395**, 33 (2004).
57. W.A.D. Heer, Rev. Mod. Phys. **65**, 611 (1993).
58. B. Assadollahzadeha, P. Schwerdtfegera, J. Chem. Phys. **131**, 06430 (2009).
59. K. Koyasu, M. Mitsui, A. Nakajima, K. Kaya, Chem. Phys. Lett. **358**, 224 (2002).
60. R. Hatz, V. Hanninen, L. Halonen, J. Phys. Chem. A **118**, 5734 (2014).